Journal of the European Ceramic Society **10** (1992) 229–235

A Push-out Technique for the Evaluation of Interfacial Properties of Fiber-reinforced Materials

G. Rausch,[a] B. Meier[b] & G. Grathwohl[a]*

[a] Institut für Keramik im Maschinenbau, Universität Karlsruhe, Haid-und-Neu-Str. 7, 7500 Karlsruhe 1, Germany
[b] Institut für Werkstoffkunde II, Universität Karlsruhe, Kaiserstr. 12, 7500 Karlsruhe 1, Germany

(Received 28 November 1991; revised version received 25 January 1992; accepted 18 March 1992)

Abstract

The friction stress and the shear strength of the interfaces in fiber-reinforced composites can be calculated from load–displacement diagrams as determined in push-out tests. In this study a fiber push-out instrument was developed, which is based on the extension of a piezo-translator connected with a hard-metal tip. Both the indentation process and the acquisition of data were carried out under computer control. Poisitioning of the indenter tip over the fiber axis was achieved using a video system with a macro-objective, allowing in-situ observation of the fiber push-out process. The examined material is a single-fiber composite consisting of a SiC fiber in an aluminosilicate glass matrix. The results of the push-out experiments and the calculation of the interfacial shear strength and the interfacial friction stress are presented and compared to data described in the literature.

Der Reibungswiderstand und die Schubfestigkeit der Faser–Matrix-Grenzflächen von faserverstärkten Verbundwerkstoffen können durch Lastverschiebungsdiagramme aus einem Push-out-Versuch berechnet werden. Im Rahmen dieser Arbeit wurde ein Push-out-Gerät entwickelt, das auf der Basis der Längenausdehnung eines Piezo-Translators verbunden mit einer Hartmetallspitze arbeitet. Sowohl die Stempelsteuerung als auch die Meßdatenerfassung sind rechnergesteuert. Das Problem der Positionierung der Stempelspitze gegenüber der Faserachse wurde mittels eines Videosystems gelöst, an das ein Makroobjektiv angeschlossen wurde. Durch diese Technik ist es auch möglich, den Push-out-Prozeß zu beobachten. Das untersuchte Material ist ein Einfaser-Verbundwerkstoff bestehend aus einer SiC-Faser in einer Aluminiumsilikat-Glasmatrix. Es werden die Ergebnisse der Push-out-Versuche und die Berechnung der Grenzflächenscherfestigkeit und des Grenzflächenreibungswiderstandes dargestellt und mit Literaturwerten verglichen.

La contrainte de friction et la force de cisaillement aux interfaces fibre–matrice dans des composites renforcés par fibres peuvent être calculées sur base des diagrammes charge-déplacement relevés au cours de tests de déchaussement des fibres. Dans ce travail, un équipage de mesure du déchaussement a été mis au point. Il est basé sur le mouvement d'un capteur piézoélectrique comprenant un embout en 'métal dur'. L'ensemble du processus d'indentation et d'acquisition des données a été informatisé. Le positionnement de l'indenteur au niveau de l'axe de la fibre est réalisé grâce à un système vidéo à objectif macro, permettant l'observation, in-situ, du déchaussement de la fibre. Le matériau examiné est un composite à une seule fibre de SiC dans une matrice en verre aluminosilicaté. Les résultats des essais de déchaussement et le calcul des forces de cisaillement et des contraintes interfaciales de friction sont présentés et comparés aux résultats publiés dans la littérature.

1 Introduction

The mechanical behavior of fiber-reinforced materials is controlled by the properties of the composite components and, in particular, by the parameters of the fiber–matrix interface. In fibre-

* To whom correspondence should be addressed.

Journal of the European Ceramic Society 0955-2219/92/$5.00

reinforced composite materials with a brittle matrix, the interfacial shear strength τ_d and the interfacial friction stress τ_f are of fundamental importance. Crack resistance and the work of fracture of such composites can be optimized by tailoring interfacial properties. They reflect the bonding state (chemical, mechanical) between the fiber and the matrix. Consequently, by measuring these interfacial parameters, a better understanding concerning the correlation of the microstructure and the reinforcing mechanisms can be achieved. This also allows the control of the reinforcing mechanisms by optimizing composite microstructure. As a basis, model specimens, e.g. single-fiber composite systems, with well-defined microstructures and fabrication conditions are used. The shear strength and the friction stress of the interface of these specimens can be determined, e.g. by means of push-out tests. Experiments of this type were carried out within the framework of the present work. A push-out testing device was designed and constructed. Monofilament fiber composite specimens, i.e. a SiC fiber coated with a matrix layer made of aluminosilicate glass, were used as the investigated material.

2 Specimen Characterization

For the monofilament composites, SiC fibers (SCS-6) supplied by Textron Specialty Materials, USA, were used. This fiber was selected for reasons of (1) handling and the fact that (2) its physical properties (E, α) are well characterized and the fiber is commercially available. The fiber is fabricated by means of chemical vapor deposition of SiC on a C core.[1] A carbon layer with an intermediate silicon enrichment is applied on the outer surface.[2] The glass matrix used is produced by Schott Glaswerke, Mainz, FRG, under the trademark of Supremax. The material data of the fiber and the matrix are listed in Table 1.

The push-out results are analyzed on the basis of these material data. The monofilament composites were produced by Schott Glaswerke in the form of a circular specimen, as shown by the micrograph in Fig. 1(a).

Table 1. Material data of the SiC fiber and the aluminosilicate glass

	SiC-fiber (SCS-6)	*Alumino silicate glass (Supremax)*[3]
Diameter (μm)	134 ± 5	—
Young's modulus (GPa)	388	87
Poisson's ratio	0·2[4]	0·24
Density (g/cm^3)	3·11	2·57
Coefficient of thermal expansion ($\times 10^{-6}$ K^{-1})	4·3[5]	4·61

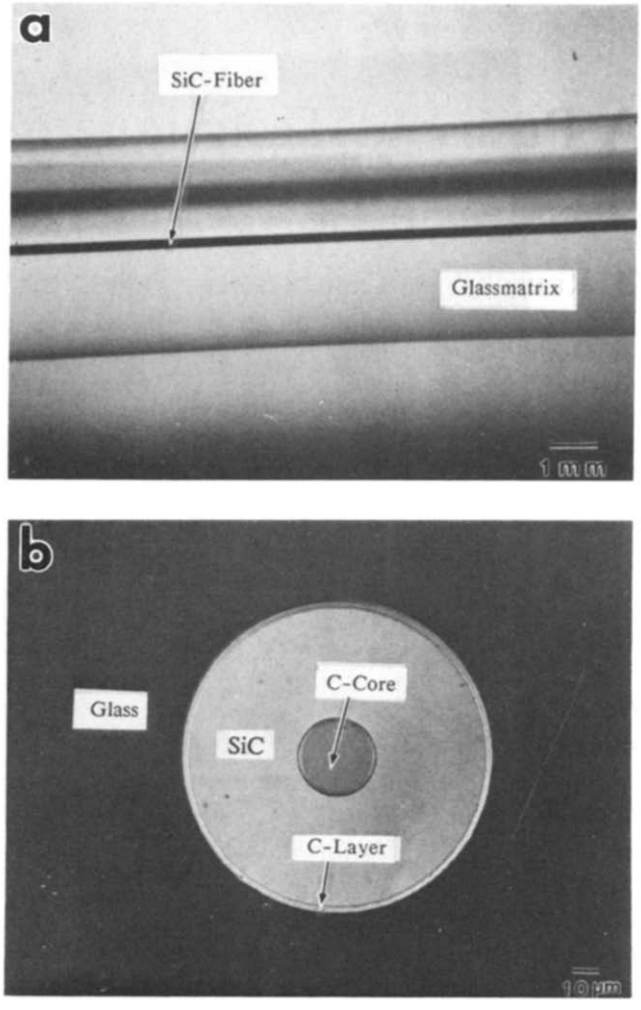

Fig. 1. General view (a) and cross-cut (b) of the single-fiber composite model specimen (light microscopy).

The light microscopy of the cross-cut of the model specimen is represented in Fig. 1(b). The microstructure of the specimen is clearly visible: glass matrix–SiC–C core. Light and scanning electron microscopy as well as high-resolution Auger spectroscopic investigations revealed that the fiber, especially its surface layers, passed through the fabrication process without any dramatic changes of the chemical and microstructural state.

3 Experimental Setup

Conventional universal testing machines are often unsuitable for performing fiber push-out tests, for failing one of the following criteria:

—Low forces have to be measured with high accuracy;

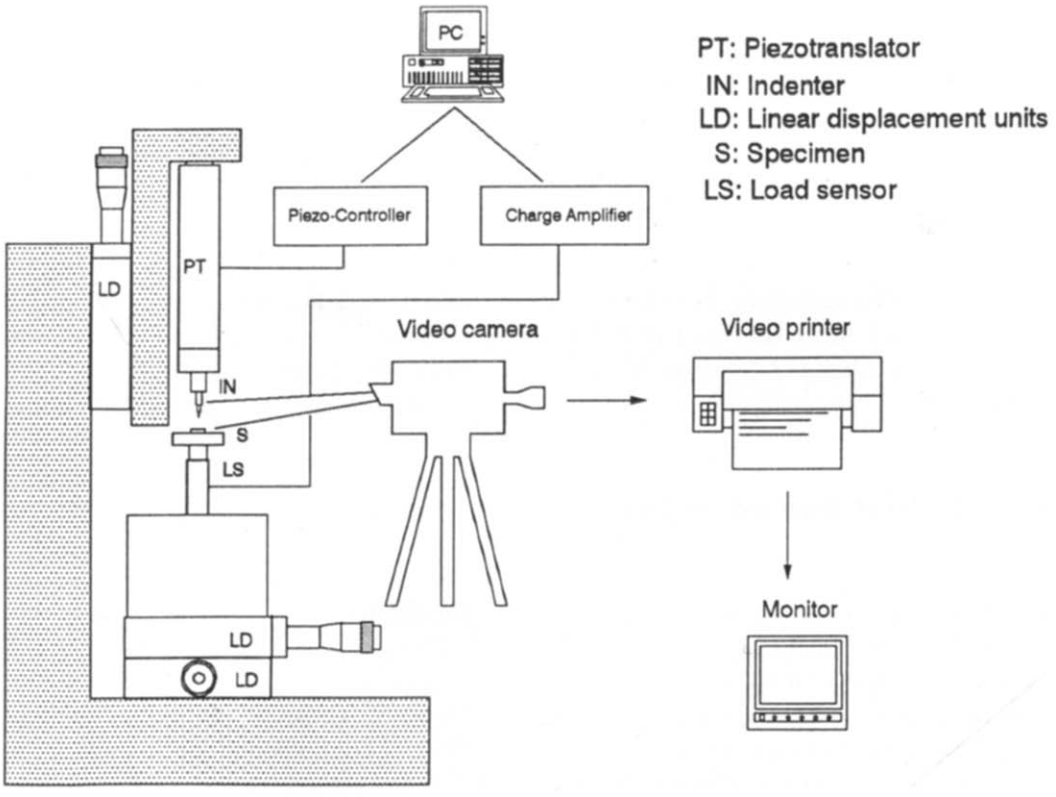

Fig. 2. Schematic representation of the testing facility.

—small indenter displacements are provided at a constant loading rate;
—exact positioning of the indenter along the central axis of the fiber has to be achieved.

A testing device meeting the above requirements was designed, constructed and installed. The individual components selected differ considerably from those of the push-out testing facilities described in the literature.[4,6,7] The small test forces arising are measured using a quartz force transducer, the measuring range of which can be adapted to any maximum load expected. The axial displacement of the indenter is achieved by means of a piezo-translator.

The hard-metal indenter tip is positioned above the fiber by means of a video camera with a macro-objective and linear displacement units. Using the piezo-translator, a vertical movement of the indenter up to a maximal nominal extension of 80 μm can be attained. The reactive forces generated are measured by a force transducer located below the specimen and passed on to the output unit. It is therefore referred to as a displacement-controlled loading device. In order to maximize machine stiffness, the complete device is mounted on a massive cast-iron angle support.

The experimental setup is represented schematically in Fig. 2. The linear displacement units have a maximum displacement of 18 mm and a setting accuracy of 1 μm. The response level of the force transducer and the resolution limit of the charge amplifier are below 1 mN. The indenter tip is made of tungsten carbide hard metal. It is a cone with a flat face of about 60 μm. Thus, a plane force-introducing surface is achieved, as a result of which a uniform surface pressure is applied to the transverse cross-section of the fiber surface. The inaccuracy of the piezo-translator is below 0·8%. Both the indent

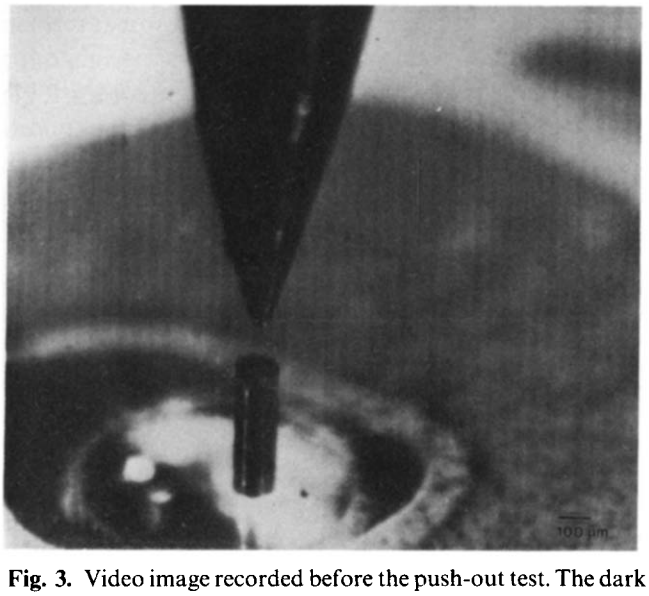

Fig. 3. Video image recorded before the push-out test. The dark cylinder shows the fiber with the indenter tip above. The dark circle below the fiber shows the bore ($d = 0{\cdot}7$ mm) in the sample holder. The glass matrix ($D = 5{\cdot}3$ mm) is transparent.

process and the acquisition of the measured data are carried out under computer control. Positioning of the indenter tip and the test control was achieved by using a video system connected with a macro-objective. The video image recorded during positioning is shown in Fig. 3. The conic indenter tip in the upper part and the SiC fiber (SCS-6) enclosed by the glass matrix in the center are clearly visible. The dark circle below the fiber represents the bore in the sample holder. This bore has a diameter of 0·7 mm. Through the bore the fiber can emerge from the composite specimen.

4 Results of the Push-out Tests and Analysis

The interfacial shear strength τ_d as measured in the push-out test is the maximum shear stress encountered at the fiber–matrix interface just prior to the first maximum in force (P_d). In contrast to this, the interfacial friction stress τ_f describes the reactive force during fiber slip opposite to the moving direction. For the determination of both interface parameters (τ_d, τ_f) different models have been developed which can be used to describe the processes taking place at the interface during the push-out test.

The model for the determination of τ_d dates back to Greszczuk[8] and was also used by Lawrence[9] for the evaluation of pull-out tests. In this case, the interface is assumed to be 'intact', i.e. no fiber slip occurs. As a consequence, this approach applies only to reversible loadings of the interface. It considers the first increase in force in the load versus indenter displacement diagram of the push-out test prior to debonding. On the side of the matrix, an interface between the fiber and the matrix is assigned to the composite specimen in the radial direction. This interface (thickness b_i, shear modulus G_i) is exposed to the shear load.

Taking into account the axial fiber elongation and the shear stress at the interface, the equilibrium of forces of the free-cut fiber volume element gives:

$$P_d = \frac{\tau_d \cdot 2\pi R}{\alpha} \cdot \tanh \alpha L \tag{1}$$

where

$$\alpha = \sqrt{\frac{2G_i}{b_i R E_f}}$$

Here P_d denotes the maximum indenter force which is just tolerated by the composite before the bonding between the fiber and the matrix is destroyed and fiber sliding occurs. R is the fiber radius, L the specimen thickness and E_f denotes Young's modulus of the fiber.

The model used for the determination of τ_f was first developed by Shetty and co-workers[7] and differs considerably from the model just described. In contrast to the method proposed by Greszczuk, fiber sliding is taken into account. In addition, the radial deformation of the fiber under load is also taken into account. It is further assumed that a radial residual stress σ_0 exists in the composite at room temperature. This residual stress is mainly caused by the different thermal expansion coefficient of the fiber ($\alpha_{th,f}$) and the matrix ($\alpha_{th,m}$). If $\alpha_{th,m} > \alpha_{th,f}$, a radial compressive strain exists after a sufficiently slow cooling from fabrication temperature to room temperature. Using the coefficient of sliding friction, μ, Coulomb's law of friction is valid for the interfacial friction stress:

$$\tau_f = \mu \cdot \sigma_0 \tag{2}$$

Here, σ_0 denotes the radial residual stress at the fiber–matrix interface.

If the transverse elongation is the same, both in the fiber and in the matrix, the axial stress of the fiber amounts to:

$$\sigma_{z,f}(z) = \frac{1}{k} \cdot \left[\left(\sigma_0 + k \cdot \frac{P}{\pi R^2} \right) \cdot \exp\left(-\frac{2\mu k z}{R} \right) - \sigma_0 \right] \tag{3}$$

where P = axial force applied to the fiber by means of the indenter, σ_0 = radial residual stress at the interface, R = fiber radius, and

$$k = \frac{\nu_f E_m}{E_f(1 + \nu_m)}$$

where E_m and ν_m = Young's modulus and the Poison's ratio of the matrix, respectively.

It is indicated by this equation that the axial stress $\sigma_{z,f}$ applied by the external force P decreases exponentially.

The distance from the fiber surface $z = l$ at which $\sigma_{z,f}$ is reduced to zero is defined as the sliding length l:

$$l = \frac{R}{2\mu k} \ln\left(\frac{\sigma_0 + kP}{\sigma_0} \right) \tag{4}$$

If the axial stress of the fiber equals zero, no fiber sliding can take place.

The maximum force tolerated by the composite during fiber sliding, P_{max}, is the force at which the sliding length l attains the specimen thickness L. P_{max} cannot be increased any further, as the fiber now

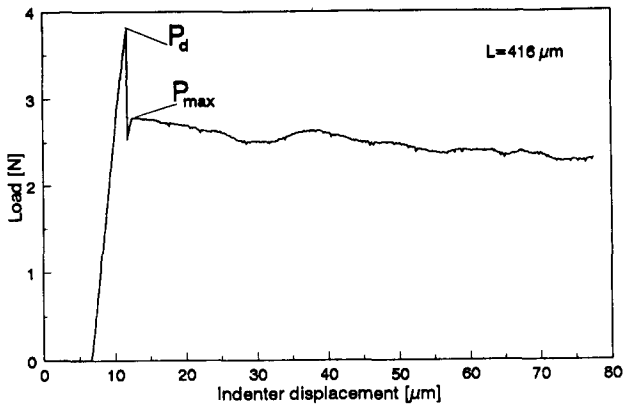

Fig. 4. Load versus displacement diagram of the thin specimen.

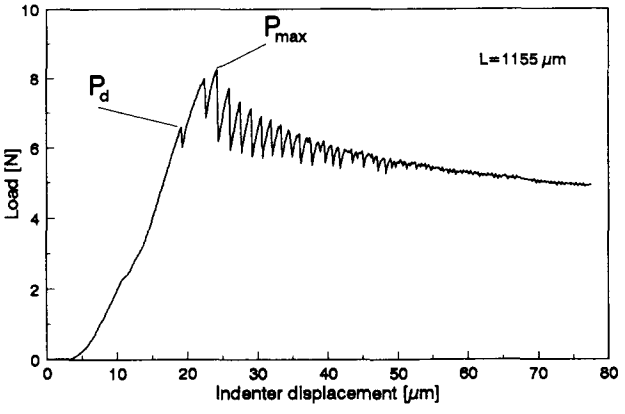

Fig. 5. Load versus displacement diagram of the thick specimen.

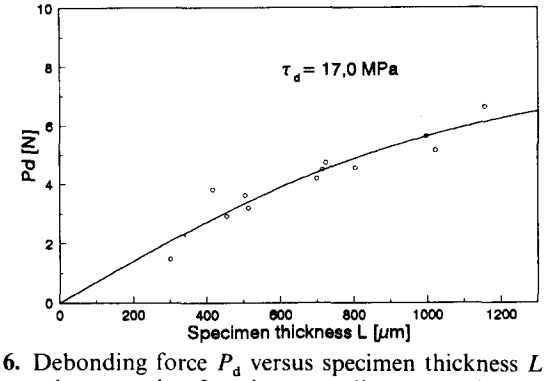

Fig. 6. Debonding force P_d versus specimen thickness L with the regression function according to eqn (1).

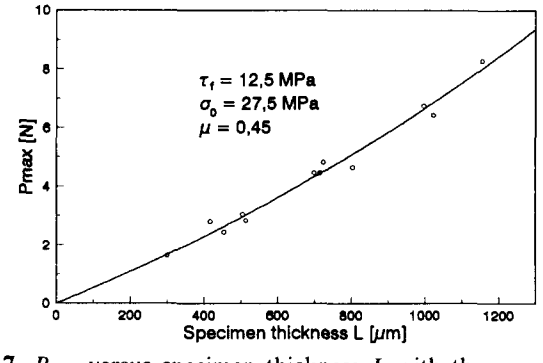

Fig. 7. P_{max} versus specimen thickness L with the regression function according to eqn (5).

begins to emerge from the opposite surface of the specimen. Hence,

$$P_{max} = \bar{P} \cdot (\exp(\lambda \cdot L) - 1) \tag{5}$$

where

$$\bar{P} = \frac{\pi R^2 \sigma_0}{k}$$

$$\lambda = \frac{2\mu k}{R}$$

$$k = \frac{v_f E_m}{E_f(1 + v_m)}$$

On the basis of these equations, the interface parameters σ_0 and μ can be determined from a series of push-out tests with specimens of variable thickness L by means of iterative regression.

For the determination of the interface parameters τ_d and τ_f, a series of push-out tests with specimens of variable thickness L is required. The results available have been obtained from a test series of 10–15 tests with a specimen thickness ranging from 300 to 1200 μm. Until now, the lower limit of 300 μm is given for reasons of preparation technology exclusively. The upper limit of L is given by the fact that the fiber sliding must be ensured over the complete specimen thickness of $L \approx 1200\,\mu$m used here. The pushing-out of the fiber at the opposite specimen surface could always be achieved. During the tests it was found that the load versus indenter displacement diagrams of thick ($L \approx 1200\,\mu$m) and thin ($L \approx 300\,\mu$m) specimens differ considerably. The diagrams are shown in Figs 4 and 5, respectively.

When comparing both diagrams it is found that

—the load P_d by far exceeds P_{max} of the thin specimen;

—the load is decreased considerably after attaining P_d in the thin specimen. This may be due to fiber roughness or variations in the fiber diameter, which has a greater influence in the case of the thick specimen.

In Figs 6 and 7, the regression adaption of P_d and P_{max} are represented for a test series with 12 specimens. The individual points describe the respective results of the push-out tests, whereas the line represents the regression function. This regression function is obtained by means of the Gauss method of least squares. The procedure is described in Ref. 4. The calculation of the interfacial properties leads to $\mu = 0{\cdot}45$, $\sigma_0 = 27{\cdot}5$ MPa, $\tau_f = 12{\cdot}5$ MPa and $\tau_d = 17{\cdot}0$ MPa.

Both figures show that the regression curves fit the measured values rather well. The degree of fitting

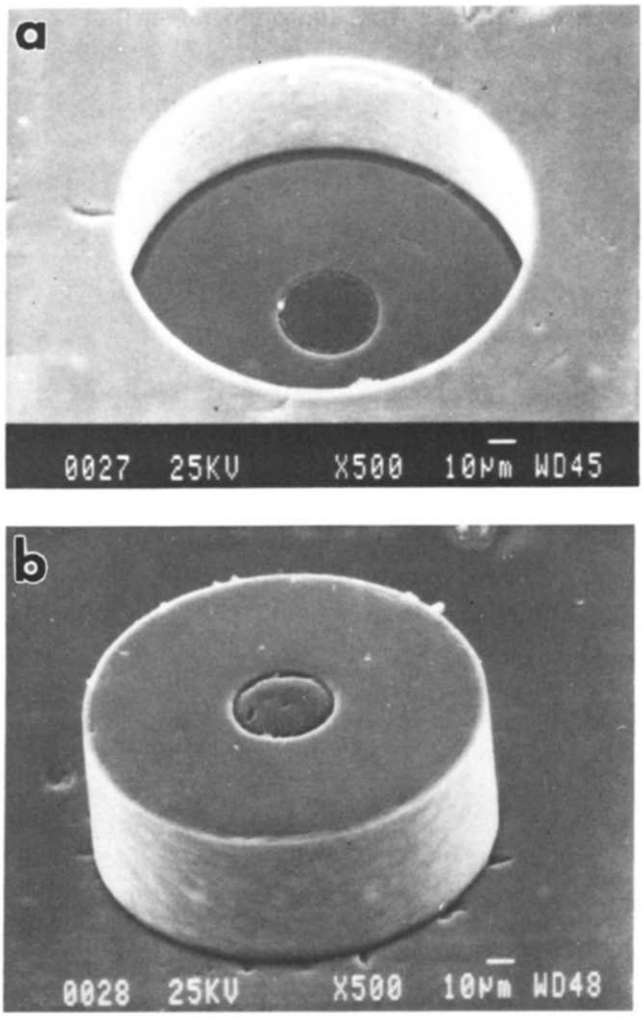

Fig. 8. Top (a) and bottom (b) of a specimen after the experiment (SEM).

can be expressed by q, which is the square of the sum of the deviations of the regression value and the measured value. For the regression curve of P_d according to eqn (1), a value of $q = 2{\cdot}26\,N^2$ for a series of 12 push-out tests was obtained. For the evaluation of P_{max} the respective value amounted to $q = 0{\cdot}83\,N^2$ (eqn (5)). Compared to the data presented by Bright *et al.*[10] ($\tau_f = 3{\cdot}01$ MPa, $\mu = 0{\cdot}047$, $\sigma_0 = 63{\cdot}6$ MPa for a monofilament composite AVCO SCS6, borosilicate glass), the shear and friction stress values obtained here are relatively high ($\tau_f = 12{\cdot}5$ MPa and $\tau_d = 17{\cdot}0$ MPa).

This might refer to the fact that the coefficient of thermal expansion (CTE) of the matrix is higher than that of the fiber, while it is smaller in the system investigated by Bright *et al.*[10] If the residual clamping stress results only from the thermal expansion mismatch of the fiber and the matrix, it can be calculated from the following equation:

$$\sigma_0 = \frac{E_m \cdot E_f \cdot \Delta\alpha \cdot \Delta T}{E_f(1 + \nu_m) + E_m(1 - \nu_f)} \qquad (6)$$

With the values given in Table 1 this equation leads to $\sigma_0 = 13{\cdot}3$ MPa. The calculation from eqn (5) yields to $\sigma_0 = 27{\cdot}5$ MPa. While eqn (6) is only suitable for sufficiently slow cooling rates it is presumed that a high cooling rate from fabrication to room temperature leads to additional stresses at the fiber–matrix interface. Further examinations to prove this presumption are in preparation.

Post-experimental examination of the push-out specimens was carried out by means of scanning electron microscopy. The top and bottom of the specimen (thickness 715 µm) are shown in Fig. 8. The fiber can be clearly seen to have been pressed into the matrix and pushed out of it at the bottom. Moreover, there is no trace of indenter penetration to be found in the fiber. The layered structure of the fiber is shown in Fig. 8(a). The outside C layer of the fiber still exists. This leads to the conclusion that the sliding between the fiber and the matrix has taken place at the outer surface of the C layer. This is also confirmed by other re-examined specimens.

5 Concluding Remarks

The design of the testing device presents a technical novelty. For the first time, a testing device for indenter tests has been developed and constructed by means of piezo-control technology. The piezo-translator proved to be very suitable. Using this translator, small distances to be controlled with a high accuracy and small outside dimensions are ensured. Computer control of the indenting process can be achieved. For the required push-out tests an exact load measurement is of a crucial importance. This is also shown to be achieved here by considering the small values of q for the square sum of the regression analysis compared to the data given in literature. While values of $q = 19\,N^2$ were presented by Bright *et al.*,[4] a value of $q = 0{\cdot}83\,N^2$ and $q = 2{\cdot}26\,N^2$, respectively, was obtained using the above experimental setup. Both the test conduct and the monitoring are facilitated considerably by a video camera. At all specimen thicknesses applied, the fiber was pushed out of the bottom of the specimen. Thus, friction during the push-out test is less affected by fluctuations of the fiber diameter. The advantage of relatively thin specimens (<700 µm) is that small test forces are sufficient to achieve a fiber sliding over the complete interface. Thus, damage of the fiber by the indenter is avoided. The testing device presented here allows a cost-effective quantitative description of the interface properties of fiber-reinforced materials to be made.

Acknowledgements

The authors would like to thank Schott Glaswerke, Mainz, for producing the composites, especially Dr Spallek, Dr Pannhorst and Dipl.-Ing. Krolla. The financial support of parts of this work by BMFT, Bundesministerium für Forschung und Technologie, is also gratefully acknowledged.

References

1. De Bolt, H. E., Krukonis, V. J. & Wawner, F. E., High strength, high modulus silicon carbide filament via chemical vapor deposition. In *Proceedings of the Third International Conference on Silicon Carbide*, University of South Carolina Press, Columbia, SC, 1973, pp. 168–75.
2. Foltz, T. F., SiC fibres for advanced ceramic composites. AVCO Speciality Materials Division, Lowell, MA.
3. Product Information, Schott Glaswerke, Mainz, FRG, 1982.
4. Bright, J. D., Shetty, D. K., Griffin, C. W. & Limaye, S. Y., Interfacial bonding and friction in SiC (filament)-reinforced ceramic and glass matrix composites. *J. Am. Ceram. Soc.*, **72** (1989) 1891–8.
5. DiCarlo, J. A., Creep of chemically vapour-deposited SiC fibres. *J. Mat. Sci.*, **21** (1986) 217–24.
6. Grande, D. H., Mandell, J. F. & Hong, C. C., Fiber–matrix bond strength studies of glass, ceramic and metal matrix composites. *J. Mat. Sci.*, **23** (1988) 311–28.
7. Shetty, D. K., Shear-lag analysis of fiber push-out (indentation) tests for estimating interfacial friction stress in ceramic–matrix composites. *J. Am. Ceram. Soc.*, **71** (1988) C-107–C-109.
8. Greszczuk, L. B., Theoretical studies of the mechanics of the fiber–matrix interface in composites. In *Interfaces in Composites, ASTM STP 452*, American Society for Testing and Materials, 1969, pp. 42–58.
9. Lawrence, P., Some theoretical considerations of fiber pull-out from an elastic matrix. *J. Mat. Sci.*, **7** (1970) 1–6.
10. Bright, J. D., Danachaivijit, S. & Shetty, D. K., Interfacial sliding friction in silicon carbide–borosilicate glass composites: a comparison of pullout and pushout tests. *J. Am. Ceram. Soc.*, **74** (1991) 115–22.